

Piezoelectric and electrostrictive contributions to optical parametric amplification of acoustic phonons in magnetized doped III-V semiconductors

JYOTI GAHLAWAT^a, MANJEET SINGH^{b*}, SUNITA DAHIYA^a

^a*Department of Physics, Baba Mastnath University, Asthal Bohar, Rohtak-124021, India*

^b*Department of Physics, Government College, Matanhai, Jhajjar – 124106, India*

In the present analytical investigation, we have explored the piezoelectric and electrostrictive contributions to optical parametric amplification of acoustic phonons in magnetized doped III-V semiconductors. Expressions are obtained for effective second-order optical susceptibility and threshold pump electric field for the onset of optical parametric amplification process. Parametric gain coefficients are obtained for different cases, viz. piezoelectric coupling only, electrostrictive coupling only, and piezoelectric and electrostrictive coupling both; well above the threshold pump field. Numerical estimates are made for n-type InSb crystal kept in an external magnetostatic field and illuminated by a pulsed CO₂ laser. The results indicate that the threshold pump field for the onset of optical parametric amplification and parametric gain coefficients can be tailored by monitoring the material parameters (such as carrier concentration, piezoelectric and/or electrostrictive coefficients), dispersion characteristics and an external magnetostatic field. It is found that proper selection of externally applied magnetostatic field reduces threshold pump field and enhances gain profile of the optical parametric amplifier. The results strongly suggest the potential of n-InSb-CO₂ laser system for the fabrication of optical parametric amplifier.

(Received November 6, 2019; accepted April 8, 2021)

Keywords: Optical parametric amplification, Piezoelectricity, Electrostriction, Acoustic phonons, III-V semiconductors

1. Introduction

The studies of parametric interaction (PI) processes play a distinctive role in nonlinear optics due to their never ending technological applications [1-4]. PI processes have been used to generate tunable coherent radiation at a frequency which is not an output of any laser source; these frequency conversion techniques give significant methods for broadening the spectral range covered by coherent sources [5, 6]. Optical harmonic generation, sum/difference frequency generation, optical parametric amplification/ oscillation/ generation, spontaneous parametric down conversion, optical Kerr effect, self focusing/ defocusing, self phase modulation, cross-phase modulation, cross-polarized wave generation etc. are some of the PI processes in a nonlinear medium. In optical parametric amplification (OPA) process, a weak signal interacts with a high frequency coherent pump wave and both the original signal as well as generated difference frequency signal (known as the idler) gets amplified. Currently, OPA is of particular interest because of its immense applications in science and technology [7, 8]. Optical parametric amplifiers have been recently used to detect weak signal at wavelengths for which sensitive sensors are not available [9].

While surveying ongoing global research activities on OPA, it has been found that the manipulations of threshold pump field and gain coefficient have been important issues to improve the efficiency and functionality of optical parametric amplifiers due to limited availability of

nonlinear optical media with desirable properties. It has been observed that among the various nonlinear media [10], especially III-V semiconductor crystals, have been regarded as most promising materials for fabrication of optoelectronic devices based on OPA [11]. In addition, in these crystals, various coherent modes such as acoustic phonon (AP) mode, optical phonon (OP) mode, polaron mode, polariton mode etc. may be excited at the expense of pump wave [12] and adopting the coupled mode approach, a strong tunable Stokes mode may be accomplished as a signal wave at the expense of pump wave.

OPA of APs in semiconductor plasma has been studied by Ghosh and Khan [13]. Gupta and Sen [14] explored the role of electrostriction on parametric dispersion and amplification of APs in doped piezoelectric semiconductors. Singh et al. [15] investigated the effects of carrier heating on parametric dispersion and amplification of AP in piezoelectric semiconductors. Lal and Aghamkar [16] studied the effect of doping concentration and a transverse magnetostatic field on threshold and gain coefficient of OPA in III-V piezoelectric semiconductors. Ghosh et al. [17] explored the role of diffusion of carriers on OPA of APs in magnetized semiconductor plasmas.

Literature survey reveals that in previously reported results, OPA of AP in III-V semiconductor crystals has been studied at length but nevertheless, the threshold value of pump electric field for the onset of OPA is observed very high and parametric gain coefficient quite low.

Keeping in mind the poor efficiency of optical parametric amplifiers, comprehensive efforts are in great demand in the modeling of important phenomenon of OPA.

It has been found that in piezoelectric semiconductors, which are natural candidates for converting mechanical energy to electrical energy or vice versa, the collective oscillation of the lattice can easily be coupled strongly with plasma wave through piezoelectricity [18]. Moreover, piezoelectricity of the medium provides the important spectral characteristics of propagation in semiconductor plasma. In this context, several features of semiconductor have been extensively explored based on piezoelectric interaction between phonons and plasmons [19]. The motivation of the present study is to obtain large parametric gain coefficient at low threshold pump field via n-InSb-CO₂ system by controlling the material parameters and/or externally applied magnetostatic field.

In highly doped semiconductors, because of the de-Broglie wavelength of plasma particles (electrons/holes) much larger than the inter-fermion distances, various quantum effects such as degeneracy pressure, electron-tunneling, Landau quantization etc. may arise [20, 21]. The disparity in nonlinear behaviour of quantum semiconductor plasmas from that of classical ones have been reported [22-24]. These investigations are based on quantum hydrodynamic (QHD) model of semiconductor plasmas. This model is useful to investigate the short-scale collective phenomena in highly doped semiconductors [25, 26]. By including the quantum diffraction terms and the statistical degeneracy pressure, QHD model becomes a generalization of the usual fluid model. Using QHD model, Ghosh et al. [27] compared the OPA characteristics of AP mode (without and with including quantum effect) in un-magnetized piezoelectric semiconductors and observed the similar nature of curves in both the cases. They found that the magnitudes of threshold pump field for the onset of OPA at $n_0 = 2 \times 10^{24} \text{ m}^{-3}$ are $9.109 \times 10^6 \text{ Vm}^{-1}$ when quantum effects are excluded and $2.086 \times 10^6 \text{ Vm}^{-1}$ when quantum effects are included.

Keeping in view the possible impact of piezoelectric and electrostrictive coefficients, our aim is to study OPA of APs in magnetized doped III-V semiconductors. For this we employ the well known hydrodynamic (fluid) model of semiconductor plasma. Using the coupled mode approach, parametric gain coefficients are obtained for different cases, i.e. electrostrictive coupling only, piezoelectric coupling only, and electrostrictive and piezoelectric coupling both. An externally applied magnetostatic field on doped III-V semiconductor crystal put several restrictions on the used fluid model [28, 29].

The structure of the paper is as follows: In section 2, expressions are obtained for effective second-order optical susceptibility, threshold electric field and parametric gain coefficients in a transversely magnetized semiconductor crystal using a single component fluid model. Section 3 includes the discussion of the analytical results obtained in the previous section. Section 4 enlists the important conclusions.

2. Theoretical formulations

We consider the well-known hydrodynamic model of homogeneous n-type semiconductor plasma with electrons as carriers exposed to an intense pump wave and an external magnetostatic field under thermal equilibrium satisfying the condition: $k_a l = 1$; k_a the acoustic wave number, and l the carrier mean free path. In magnetized III-V semiconductor crystals, the piezoelectric and electrostrictive coefficients are non-isotropic and hence the off-diagonal components of the susceptibility tensor are finite. For the sake of convenience, we consider generation of longitudinal AP mode in the semiconductor medium possessing $\bar{4}3m$ symmetry and for such mode the piezoelectric and electrostrictive tensor reduces to a single component [30, 31].

2.1. Effective second-order optical susceptibility

In one dimensional configuration, OPA can be described by parametric coupling among three waves:

(i) the input strong pump beam field $\xi_0(x, t) = \xi_0 \exp[i(k_0 x - \Omega_0 t)]$,

(ii) the AP mode $u(x, t) = u_0 \exp[i(k_a x - \Omega_a t)]$, and

(iii) the scattered Stokes component of pump wave field $\xi_s(x, t) = \xi_s \exp[i(k_s x - \Omega_s t)]$.

The momentum and energy exchange between these waves can be described by phase matching conditions:

$$\hbar \vec{k}_0 = \hbar \vec{k}_s + \hbar \vec{k}_a \quad (\text{momentum conservation relation})$$

$$\hbar \Omega_0 = \hbar \Omega_s + \hbar \Omega_a \quad (\text{energy conservation relation}).$$

The time varying pump field produces piezoelectric strain (via first-order forces) and electrostrictive strain (via second-order forces) and thus derives an AP mode in the crystal. The induced strains modulate the optical dielectric constant and cause an energy exchange between pump and scattered waves. Let the deviation of a point x from its mean position be $u(x, t)$, so that the one-dimensional strain is $\frac{\partial u}{\partial x}$.

The first- and second-order forces acting along x -axis in terms of piezoelectric (β) and electrostrictive (γ) coefficients can be expressed as $\beta \frac{\partial \xi_a}{\partial x}$ and $\frac{\gamma}{2} \frac{\partial}{\partial x} (\xi_0 \xi_s^*)$ respectively.

The equation of motion for $u(x, t)$ of lattice vibrations due to process of piezoelectricity and electrostriction in the presence of magnetostatic field can be expressed as

$$\rho \frac{\partial^2 u}{\partial t^2} = C \frac{\partial^2 u}{\partial x^2} + \beta \frac{\partial \xi_a}{\partial x} + \frac{\gamma}{2} \frac{\partial}{\partial x} (\vec{\xi}_e \cdot \vec{\xi}_s^*) - 2\Gamma_a \rho \frac{\partial u}{\partial t} \quad (1)$$

where $\vec{\xi}_e = \vec{\xi}_0 + (\vec{v}_0 \times \vec{B}_0)$, \vec{v}_0 being the oscillatory fluid velocity of an electron of effective mass m and charge $-e$. $\vec{B}_0 = \hat{z}B_0$ is an external magnetostatic field. ρ , C and Γ_a are the mass density, elastic constant and

phenomenological damping parameter of the crystal, respectively.

The other basic equations of the analysis are:

$$\frac{\partial \bar{v}_0}{\partial t} + \mathbf{v} \bar{v}_0 = -\frac{e}{m} (\bar{\xi}_e) \quad (2)$$

$$\frac{\partial \bar{v}_1}{\partial t} + \mathbf{v} \bar{v}_1 + \left(\bar{v}_0 \frac{\partial}{\partial x} \right) \bar{v}_1 = -\frac{e}{m} [\bar{\xi}_1 + (\bar{v}_1 \times \bar{B}_0)] \quad (3)$$

$$\frac{\partial n_1}{\partial t} + n_0 \frac{\partial v_1}{\partial x} + n_1 \frac{\partial v_0}{\partial x} + v_0 \frac{\partial n_1}{\partial x} = 0 \quad (4)$$

$$\bar{P}_{es} = -\gamma \frac{\partial u^*}{\partial x} (\bar{\xi}_e) \quad (5)$$

$$\frac{\partial \xi_s}{\partial x} + \frac{\beta}{\varepsilon} \frac{\partial^2 u}{\partial x^2} + \frac{\gamma}{\varepsilon} \frac{\partial^2 u^*}{\partial x^2} (\xi_e) = -\frac{n_1 e}{\varepsilon} \quad (6)$$

For a detailed description of these Eqs., the reader is addressed to Ref. [15]. Here \bar{v}_0 , \bar{v}_1 , n_0 , n_1 and \mathbf{v} represent the zeroth-order oscillatory fluid velocity, first-order oscillatory fluid velocity, equilibrium electron density, perturbed electron density and electron-electron collision frequency, respectively.

The first- and second-order forces produce carrier density perturbation within the doped semiconductor crystal, which can be obtained by using the method adopted by Singh et.al. [15] as

$$\frac{\partial^2 n_1}{\partial t^2} + \mathbf{v} \frac{\partial n_1}{\partial t} + \bar{\Omega}_p^2 n_1 + \frac{n_0 e k_s^2 A_1 u^*}{m \varepsilon_1} (\xi_0 \xi_s) = i n_1 k_s \bar{\xi} \quad (7)$$

where $\bar{\xi} = \frac{e}{m} (\bar{\xi}_e)$, $\bar{\Omega}_p = \frac{\Omega_p \mathbf{v}}{(\mathbf{v}^2 + \Omega_c^2)^{1/2}}$,

$$A_1 = \frac{\Delta_1 \Delta_2}{\xi_0} \left(\frac{\beta^2}{\xi_0} + \beta \gamma \right), \text{ in which } \Delta_1 = 1 - \frac{\Omega_c^2}{(\Omega_0^2 - \Omega_c^2)}, \text{ and}$$

$$\Delta_2 = 1 - \frac{\Omega_c^2}{(\Omega_s^2 - \Omega_c^2)}.$$

$\Omega_c = \frac{e}{m} B_0$ (electron cyclotron frequency), and

$$\Omega_p = \left(\frac{n_0 e^2}{m \varepsilon} \right)^{1/2} \text{ (electron plasma frequency).}$$

The density perturbation n_1 oscillate at induced wave frequency components (i.e. Ω_a and Ω_s) which can be expressed as: $n_1 = n_{1s}(\Omega_a) + n_{1f}(\Omega_s)$, where n_{1s} (slow frequency component) is associated with vibrations at Ω_a and n_{1f} (high frequency component) oscillates at the electromagnetic wave frequencies $\Omega_0 \pm \Omega_a$. The higher-order terms with frequencies $\Omega_{s,p} (= \Omega_0 \pm p \Omega_a)$, for $p = 2, 3, \dots$, being off-resonant, are neglected.

Under rotating-wave approximation (RWA), Eq. (7) leads to the following coupled equations:

$$\frac{\partial^2 n_{1f}}{\partial t^2} + \mathbf{v} \frac{\partial n_{1f}}{\partial t} + \bar{\Omega}_p^2 n_{1f} + \frac{n_0 e k_s^2 A_1 u^*}{m \varepsilon_1} (\xi_0 \xi_s) = -i n_{1s}^* k_s \bar{\xi} \quad (8a)$$

and

$$\frac{\partial^2 n_{1s}}{\partial t^2} + \mathbf{v} \frac{\partial n_{1s}}{\partial t} + \bar{\Omega}_p^2 n_{1s} = i n_{1f}^* k_s \bar{\xi}. \quad (8b)$$

Eqs. (8a) and (8b) reveal that the density perturbation components are coupled to each other via the pump electric field. By solving simultaneous Eqs. (8a) and (8b), expressions for n_{1s} and n_{1f} can be obtained as well as their values may be determined by knowing the material parameters and electric field amplitudes. The expression for n_{1s} is obtained as

$$n_{1s} = \frac{\varepsilon_0 k_a k_s}{2 \rho \varepsilon (\Omega_{ad}^2 - 2i \Gamma_a \Omega_a)} \left(\frac{A_1}{A_2} \right) \xi_0 \xi_s^* \quad (9)$$

where $\Omega_{ad}^2 = \Omega_a^2 - k_a^2 v_a^2$ (AP dispersion),

$$A_2 = 1 - \frac{(\Omega_{ps}^2 - i v \Omega_s)(\Omega_{pa}^2 + i v \Omega_a)}{k_s^2 \xi^2}, \text{ in which } \Omega_{ps}^2 = \bar{\Omega}_p^2 - \Omega_s^2$$

and $\Omega_{pa}^2 = \bar{\Omega}_p^2 - \Omega_a^2$.

The backward Stokes component of the nonlinear current density can be given as $J_{nl}(\Omega_s) = n_{1s}^* e v_0$

$$= \frac{k_a k_s \Omega_p^2 (\mathbf{v} - i \Omega_0)}{2 \rho (\Omega_{ad}^2 - 2i \Gamma_a \Omega_a) (\Omega_c^2 - \Omega_0^2)} \left(\frac{A_1}{A_2} \right) \xi_0 \xi_s^* \quad (10)$$

The time integral of the nonlinear current density yields the induced nonlinear polarization as

$$P_{cd}(\Omega_s) = \int J_{nl}(\Omega_s) dt = \frac{k_a k_s \Omega_p^2 \Omega_0^3}{2 \rho \Omega_s (\Omega_{ad}^2 - 2i \Gamma_a \Omega_a) (\Omega_c^2 - \Omega_0^2)} \left(\frac{A_1}{A_2} \right) \xi_0 \xi_s^* \quad (11)$$

Comparing Eq. (11) with the well-known relation $P_{cd}(\Omega_s) = \varepsilon_0 \chi_{cd}^{(2)} \xi_0 \xi_s^*$, the second-order optical susceptibility due to induced nonlinear polarization $P_{cd}(\Omega_s)$ is given by

$$\chi_{cd}^{(2)} = \frac{k_a k_s \Omega_p^2 \Omega_0^3}{2 \rho \varepsilon_0 \Omega_s (\Omega_{ad}^2 - 2i \Gamma_a \Omega_a) (\Omega_c^2 - \Omega_0^2)} \left(\frac{A_1}{A_2} \right) \quad (12)$$

In addition to $P_{cd}(\Omega_s)$, the medium should also possess electrostrictive polarization $P_{es}(\Omega_s)$ arising due to the interaction of pump wave with the generated AP mode in the medium. The electrostrictive polarization is obtained from Eqs. (1) and (5) as

$$P_{es}(\Omega_s) = \frac{k_a k_s \Omega_0^4 \gamma^2 \xi_0 \xi_s^*}{2 \rho (\Omega_{ad}^2 - 2i \Gamma_a \Omega_a) (\Omega_c^2 - \Omega_0^2)^2} \quad (13)$$

Comparing Eq. (13) with the well known relation $P_{es}(\Omega_s) = \epsilon_0 \chi_{es}^{(2)} \xi_0 \xi_s^*$, the second-order optical susceptibility due to electrostrictive polarization $P_{es}(\Omega_s)$ is given by

$$\chi_{es}^{(2)} = \frac{k_a k_s \Omega_0^4 \gamma^2}{2\rho \epsilon_0 (\Omega_a^2 - 2i\Gamma_a \Omega_a)(\Omega_c^2 - \Omega_0^2)} \quad (14)$$

Using Eqs. (12) and (14), the effective second-order optical susceptibility $\chi_{eff}^{(2)}$ is given as $\chi_{eff}^{(2)} = \chi_{cd}^{(2)} + \chi_{es}^{(2)}$

$$= \frac{k_a k_s \Omega_0^4}{2\rho \epsilon_0 (\Omega_{ad}^2 - 2i\Gamma_a \Omega_a)(\Omega_c^2 - \Omega_0^2)} \left[\frac{\Omega_p^2}{\Omega_s \Omega_0} \left(\frac{A_1}{A_2} \right) + \gamma^2 \right] \quad (15)$$

Rationalization of Eq. (15) yields the imaginary part of effective second-order optical susceptibility as

$$[\chi_{eff}^{(2)}]_i = \frac{k_a k_s \Omega_0^4 \Omega_a \Gamma_a}{2\rho \epsilon_0 (\Omega_{ad}^4 + 4\Gamma_a^2 \Omega_a^2)(\Omega_c^2 - \Omega_0^2)} \times \left[\frac{\Omega_p^2 \Delta_1 \Delta_2}{\Omega_s \Omega_0 A_2 \xi_0} \left(\frac{\beta^2}{\xi_0} + \beta\gamma \right) + \gamma^2 \right] \quad (16)$$

2.2. Threshold pump electric field for the onset of OPA

The threshold pump electric field $\xi_{0,th}$ for the onset of OPA process, which is necessary condition for parametric gain to occur, can be obtained by putting $[\chi_{eff}^{(2)}]_i = 0$ in Eq. (16) as

$$\xi_{0,th} = \frac{m}{ek_s} \left(1 - \frac{\Omega_c^2}{\Omega_0^2} \right) \left| (\Omega_{ps}^2 - i\nu\Omega_s)(\Omega_{pa}^2 + i\nu\Omega_a) \right|^{1/2} \quad (17)$$

Eq. (17) reveals that $\xi_{0,th}$ is independent of type of coupling (electrostrictive, piezoelectric or both) for the occurrence of OPA process. Therefore the interaction between pump and magnetized semiconductor crystal will be dominated by the parametric phenomena at a pump electric well above the threshold field (i.e. $\xi_0 > \xi_{0,th}$).

2.3. Parametric gain coefficients

In order to obtain the parametric gain coefficient g_{para} in a magnetized doped III-V semiconductor crystal, we employ the relation [15]:

$$g_{para} = \frac{\Omega_s}{\eta c} [\chi_{eff}^{(2)}]_i \quad (18)$$

The parametric gain of the signal as well as the idler waves is possible only if g_{para} is negative for pump field $|\xi_0| > |\xi_{0,th}|$.

Eq. (18) can be used to obtain parametric gain coefficient for different cases of interest.

(i) Piezoelectric and electrostrictive coupling both ($\beta, \gamma \neq 0$):

$$(g_{para})_{\beta, \gamma \neq 0} = \frac{k_a k_s \Omega_0^4 \Omega_a \Gamma_a}{2\rho \epsilon_0 (\Omega_{ad}^4 + 4\Gamma_a^2 \Omega_a^2)(\Omega_c^2 - \Omega_0^2)} \times \left[\frac{\Omega_p^2 \Delta_1 \Delta_2}{\Omega_s \Omega_0 A_2 \xi_0} \left(\frac{\beta^2}{\xi_0} + \beta\gamma \right) + \gamma^2 \right] \quad (18a)$$

(ii) Electrostrictive coupling only ($\beta = 0, \gamma \neq 0$):

$$(g_{para})_{\beta=0, \gamma \neq 0} = \frac{k_a k_s \Omega_0^4 \Omega_a \Gamma_a \gamma^2}{2\rho \epsilon_0 (\Omega_{ad}^4 + 4\Gamma_a^2 \Omega_a^2)(\Omega_c^2 - \Omega_0^2)} \quad (18b)$$

(iii) Piezoelectric coupling only ($\beta \neq 0, \gamma = 0$):

$$(g_{para})_{\beta \neq 0, \gamma = 0} = \frac{k_a k_s \Omega_0^3 \Omega_a \Omega_p^2 \Gamma_a \Delta_1 \Delta_2 \beta^2}{2\rho \epsilon_0 \Omega_s A_2 \xi_0^2 (\Omega_{ad}^4 + 4\Gamma_a^2 \Omega_a^2)(\Omega_c^2 - \Omega_0^2)} \quad (18c)$$

3. Results and discussion

To have a numerical appreciation of the results obtained in the analysis, we assumed n-type InSb crystal with electron effective mass $m = 0.0145m_e$ (m_e being the rest mass of electron), as the representative III-V semiconductor crystal. It is assumed to be illuminated by 10.6 μm ($\Omega_0 = 1.78 \times 10^{14} \text{ s}^{-1}$) pulsed CO₂ laser. The other parameters are given in Table 1 [15].

Table 1. Material parameters of n-InSb crystal at 77 K

Mass Density ρ (kg m ⁻³)	Piezoelectric coefficient β (C m ⁻²)	Electrostriction coefficient γ (s ⁻¹)	Acoustic damping parameter Γ_a (s ⁻¹)	Acoustic wave velocity v_a (ms ⁻¹)	Acoustic wave frequency Ω_a (s ⁻¹)	Electron collision frequency ν (s ⁻¹)
5.8×10^3	0.054	5×10^{-10}	2×10^{10}	4×10^3	2×10^{11}	4×10^{11}

The main focus of this paper is to study the threshold characteristics for the onset of OPA and parametric gain coefficients in transversely magnetized doped III-V semiconductors. We consider the wide range of doping concentration ($10^{19} \text{ m}^{-3} < n_0 < 10^{24} \text{ m}^{-3}$) and externally applied magnetostatic field ($0 < B_0 < 18 \text{ T}$). The magnetostatic field applied on III-V semiconductor in this range is feasible. Here, it should be mentioning that Generazio and Spector [32] developed the theoretical formulation of free carrier absorption for n-InSb-CO₂ and n-InSb-CO laser systems at 77 K by placing the sample in an external magnetostatic field $B_0 \leq 20 \text{ T}$.

3.1. Threshold characteristics for the onset of OPA

Using the material parameters (for n-InSb) given in Table 1, the variation of threshold pump amplitude $\xi_{0,th}$ for the onset of OPA on different parameters such as acoustic wave number k_a , magnetostatic field B_0 (introduced via cyclotron frequency Ω_c), doping concentration n_0 (introduced via plasma frequency Ω_p) etc. may be studied from Eq. (17). The results are plotted in Figs. 1-3.

Fig. 1 shows the variation of $\xi_{0,th}$ with k_a for $n_0 \approx 10^{22} \text{ m}^{-3}$ and $B_0 = 14.2 \text{ T}$ (because at this particular value of B_0 , $\Omega_c \sim \Omega_0$ and the factor $\left(1 - \frac{\Omega_c^2}{\Omega_0^2}\right) \rightarrow 0$ in Eq. (17), which lowers $\xi_{0,th}$). It can be inferred from this figure that $\xi_{0,th}$ is very sensitive to the dispersion characteristics of acoustic wave.

In anomalous dispersion regime ($\Omega_a > k_a v_a$) of the acoustic wave, $\xi_{0,th}$ decreases rapidly; whereas in normal dispersion regime ($\Omega_a < k_a v_a$) of acoustic wave, $\xi_{0,th}$ remains nearly constant. However, as we approach the dispersion-less regime ($\Omega_a \approx k_a v_a$), $\xi_{0,th}$ decreases very sharply acquiring a minimum value ($\xi_{0,th} = 5 \times 10^6 \text{ Vm}^{-1}$) in the presence of non-dispersive acoustic wave ($\Omega_a = k_a v_a$). Hence lowest $\xi_{0,th}$ can be obtained in the dispersion-less regime of acoustic wave.

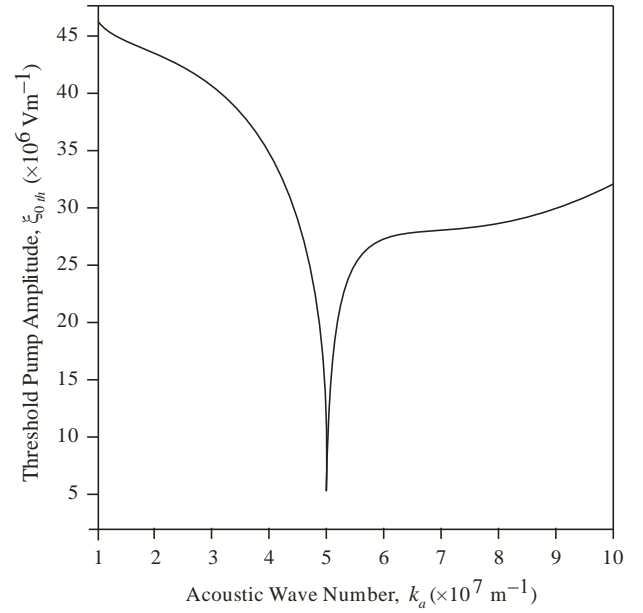


Fig. 1. Variation of threshold pump amplitude $\xi_{0,th}$ with acoustic wave number k_a for $n_0 \approx 10^{22} \text{ m}^{-3}$, $B_0 = 14.2 \text{ T}$

Fig. 2 shows the variation of $\xi_{0,th}$ with B_0 for $n_0 \approx 10^{22} \text{ m}^{-3}$ for different cases, viz. anomalous ($\Omega_a > k_a v_a$), normal ($\Omega_a < k_a v_a$), and dispersion-less ($\Omega_a \approx k_a v_a$) regimes of the acoustic wave. It can be observed that in all the three cases, $\xi_{0,th}$ starts with a high value at in the absence of B_0 ; remains nearly constant for $B_0 \leq 10 \text{ T}$ and decreases sharply attaining a minimum value ($\xi_{0,th} = 5.4 \times 10^6 \text{ Vm}^{-1}$) at $B_0 \approx 11 \text{ T}$. With increasing B_0 beyond this value, $\xi_{0,th}$ increases sharply and remains constant over a narrow range of B_0 ($\approx 11 - 13 \text{ T}$). With further increasing B_0 , $\xi_{0,th}$ again decreases sharply attaining a minimum value ($\xi_{0,th} = 1.6 \times 10^6 \text{ Vm}^{-1}$) at $B_0 = 14.2 \text{ T}$. Beyond this value of B_0 , $\xi_{0,th}$ shoots up. The dip at $B_0 \approx 11 \text{ T}$ and 14.2 T may be attributed to resonance conditions: $\Omega_c \sim \Omega_s$ (via parameter Ω_{ps}^2) and $\Omega_c \sim \Omega_0$ (via parameter $\left(1 - \frac{\Omega_c^2}{\Omega_0^2}\right)$), respectively. Around these

resonance conditions, the drift velocity of electrons (which is also a function of magnetostatic field) in III-V semiconductor crystal becomes much greater than the AP mode velocity and because of this more there is a transfer of extra energy from electron-plasma wave to AP mode, and eventually the AP mode amplifies. In turn, the amplified AP mode strongly interacts with the pump wave and as a result of this the scattered Stokes mode field strength enhances largely, thereby reducing $\xi_{0,th}$. While at off-resonant conditions, fluctuations in electron

concentration in semiconductor crystal causes damping of AP mode thereby decreasing the rate of energy transfer from electron-plasma wave to AP mode, finally leading to larger $\xi_{0,th}$.

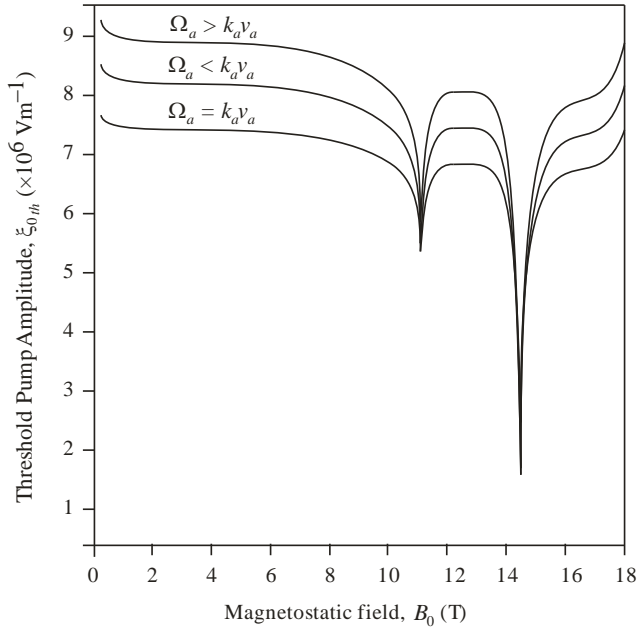


Fig. 2. Variation of threshold pump amplitude $\xi_{0,th}$ with externally applied magnetostatic field B_0 for $n_0 \approx 10^{22} \text{ m}^{-3}$

A comparison among the three cases reveals that except $B_0 \approx 11 \text{ T}$ and 14.2 T ,

$$(\xi_{0,th})_{\Omega_a > k_a v_a} > (\xi_{0,th})_{\Omega_a < k_a v_a} > (\xi_{0,th})_{\Omega_a = k_a v_a}$$

Particularly, at $B_0 \approx 11 \text{ T}$ and 14.2 T , $\xi_{0,th}$ becomes independent of dispersion characteristics of acoustic wave.

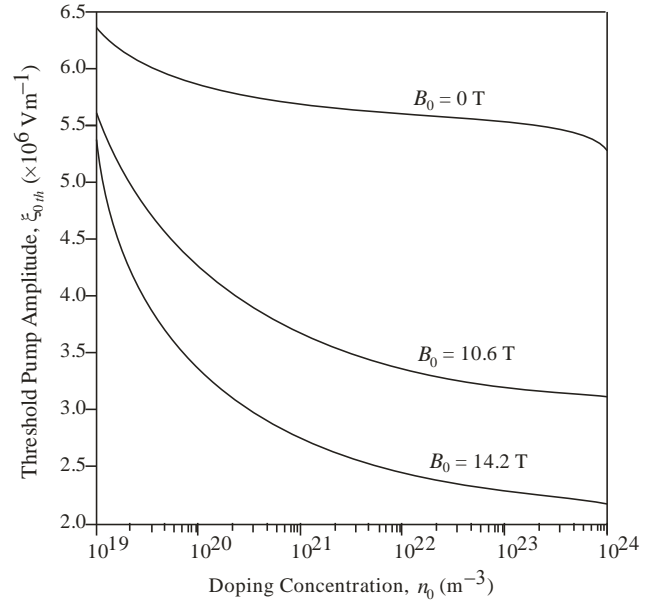


Fig. 3. Variation of threshold pump amplitude $\xi_{0,th}$ with doping concentration n_0

Fig. 3 shows the variation of $\xi_{0,th}$ with n_0 for different cases, viz. absence of magnetostatic field ($B_0 = 0 \text{ T}$), and presence of magnetostatic field ($B_0 \approx 11 \text{ T}$, 14.2 T). Here we considered two particular values of magnetostatic field ($B_0 \approx 11 \text{ T}$, 14.2 T) because at these two values of B_0 , $\xi_{0,th}$ is lowest as suggested from Fig. 2. We observed that in all the cases, $\xi_{0,th}$ is relatively higher in lightly doped regime ($n_0 \approx 10^{19} \text{ m}^{-3}$). With increasing n_0 , $\xi_{0,th}$ is higher and remains nearly constant in the absence of magnetostatic field ($B_0 = 0 \text{ T}$), while $\xi_{0,th}$ is lower and decreases parabolically in the presence of magnetostatic field ($B_0 \approx 11 \text{ T}$, 14.2 T).

Moreover, $(\xi_{0,th})_{B_0=14.2 \text{ T}} > (\xi_{0,th})_{B_0 \approx 11 \text{ T}}$. This result is well in agreement with the result of Pilak and Furdyna [33]. Here, it should be pointed out that for doping concentration $n_0 > 10^{24} \text{ m}^{-3}$, the diffusion effects are pronounced and the theory thereby needs a modification [17]. Table 2 shows the calculated values of threshold pump amplitude for the onset of OPA in n-InSb crystal.

Table 2. Calculated values of threshold pump amplitude for the onset of OPA in n-InSb crystal

Threshold pump amplitude $E_{0,th}$ (Vm^{-1})	Wave number k_a (m^{-1})	Magnetostatic field B_0 (T)	Doping concentration n_0 (m^{-3})
2×10^8	5×10^7	0	10^{22}
5.4×10^6	5×10^7	11	10^{22}
1.6×10^6	5×10^7	14.2	10^{22}

3.2. Gain characteristics of OPA

Using the material parameters (for n-InSb), given in Table 1, the nature of dependence of parametric gain coefficients due to piezoelectric coupling only $(g_{para})_{\beta,\gamma \neq 0}$, electrostrictive coupling only $(g_{para})_{\beta=0,\gamma \neq 0}$, and piezoelectric and electrostrictive coupling both $(g_{para})_{\beta \neq 0,\gamma=0}$ on different parameters such as acoustic wave number k_a , magnetostatic field B_0 (introduced via cyclotron frequency Ω_c), doping concentration n_0 (introduced via plasma frequency Ω_p), pump field amplitude ξ_0 etc. may be studied from Eqs. (18a) - (18c). The results are plotted in Figs. 4-7. In Figs. 4-6, we considered pump field amplitude $\xi_0 = 6 \times 10^7 \text{ Vm}^{-1} (> \xi_{0,th})$.

Fig. 4 shows the variation of parametric gain coefficients $((g_{para})_{\beta,\gamma \neq 0}, (g_{para})_{\beta=0,\gamma \neq 0}, (g_{para})_{\beta \neq 0,\gamma=0})$ with k_a for $n_0 \approx 10^{22} \text{ m}^{-3}$ and $B_0 = 14.2 \text{ T}$.

It can be observed that the gain coefficients are smaller in anomalous dispersion ($\Omega_a > k_a v_a$; $k_a < 5 \times 10^7 \text{ m}^{-1}$) and normal dispersion ($\Omega_a < k_a v_a$; $k_a > 5 \times 10^7 \text{ m}^{-1}$) regimes of acoustic wave. However, in dispersion-less regime ($\Omega_a = k_a v_a$; $k_a = 5 \times 10^7 \text{ m}^{-1}$) of acoustic wave, the gain coefficients shows a peak, independent of type of coupling. This behavior reflects the fact that $g_{para} \propto (\Omega_a^2 - k_a^2 v_a^2)^{-2}$ (via parameter Ω_{ad}^4 in denominator of Eqs. (18a) - (18c)). Hence, the parametric gain coefficients becomes independent of type of (piezoelectric and/or electrostrictive) coupling and enhance by properly adjusting the acoustic wave number in dispersion-less regime.

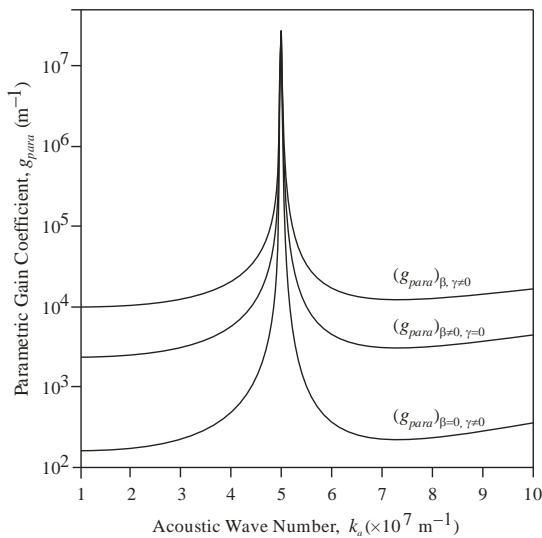


Fig. 4. Variation of parametric gain coefficients g_{para} with acoustic wave number k_a for $n_0 \approx 10^{22} \text{ m}^{-3}$ and $B_0 = 14.2 \text{ T}$

Fig. 5 shows the variation of parametric gain coefficients $((g_{para})_{\beta,\gamma \neq 0}, (g_{para})_{\beta=0,\gamma \neq 0}, (g_{para})_{\beta \neq 0,\gamma=0})$ with B_0 for $n_0 \approx 10^{22} \text{ m}^{-3}$. We observed that except for $B_0 \approx 11 \text{ T}$ and 14.2 T , the gain coefficients are relatively small and nearly independent of magnetostatic field. At $B_0 \approx 11 \text{ T}$ and 14.2 T , we observed sharp peaks in gain spectrum. The peaks at $B_0 \approx 11 \text{ T}$ and 14.2 T may be attributed to resonance conditions $\Omega_c \sim \Omega_s$ (via parameter Ω_{ps}^2) and $\Omega_c \sim \Omega_0$ (via parameter $\left(1 - \frac{\Omega_c^2}{\Omega_0^2}\right)$), respectively in confirmatory with Eqs. (18a) - (18c). A comparison between the two peaks yields the following ratio:

- (i) For $\beta \neq 0$ and $\gamma = 0$, $\frac{(g_{para})_{B=14.2\text{T}}}{(g_{para})_{B \approx 11\text{T}}} = 1.18 \times 10^2$.
- (ii) For $\beta = 0$ and $\gamma \neq 0$, $\frac{(g_{para})_{B=14.2\text{T}}}{(g_{para})_{B \approx 11\text{T}}} = 11.3$.
- (iii) For $\beta, \gamma \neq 0$, $\frac{(g_{para})_{B=14.2\text{T}}}{(g_{para})_{B \approx 11\text{T}}} = 6.15 \times 10^2$.

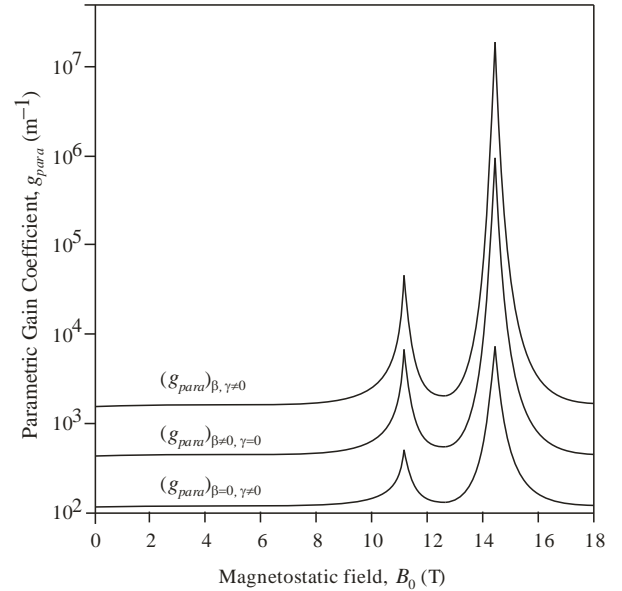


Fig. 5. Variation of parametric gain coefficients g_{para} with externally applied magnetostatic field B_0 for $n_0 \approx 10^{22} \text{ m}^{-3}$

Here, it should be pointed out that Lal and Aghamkar [16] while studying OPA in piezoelectric magnetized semiconductors observed switching of parametric negative and positive gain coefficients (i.e. absorption and amplification) at three different resonance conditions, viz. (i) acoustic wave frequency and electron-plasma frequency, (ii) Stokes wave frequency and electron-cyclotron frequency, and (iii) Stokes frequency and

modified electron-cyclotron frequency. But in the present analysis, we obtained sharp peaks of parametric coefficients at two different resonance conditions, viz. (i) electron-cyclotron frequency and Stokes wave frequency, and (ii) electron-cyclotron frequency and pump wave frequency. Thus the resonance conditions at which sharp peaks of parametric gain coefficients are obtained are quite different in both the studies. Moreover, the maximum value of parametric gain coefficient obtained in the present study is about 10 times more than that obtained by Lal and Aghamkar [16].

Fig. 6 shows the variation of parametric gain coefficients $(g_{para})_{\beta,\gamma \neq 0}$, $(g_{para})_{\beta=0,\gamma \neq 0}$, $(g_{para})_{\beta \neq 0,\gamma=0}$ with n_0 for $B_0 = 14.2T$. It can be observed that for low doping levels ($n_0 \approx 10^{19} \text{ m}^{-3}$), all the curves nearly coincide. The gain coefficients increase rapidly with increasing doping levels ($n_0 \approx 10^{22} \text{ m}^{-3}$) and finally saturating at high levels of doping ($n_0 \approx 10^{24} \text{ m}^{-3}$). Hence, the parametric gain coefficients can be enhanced significantly by n-type doping in III-V semiconductors in doping range $10^{19} \text{ m}^{-3} < n_0 < 10^{22} \text{ m}^{-3}$.

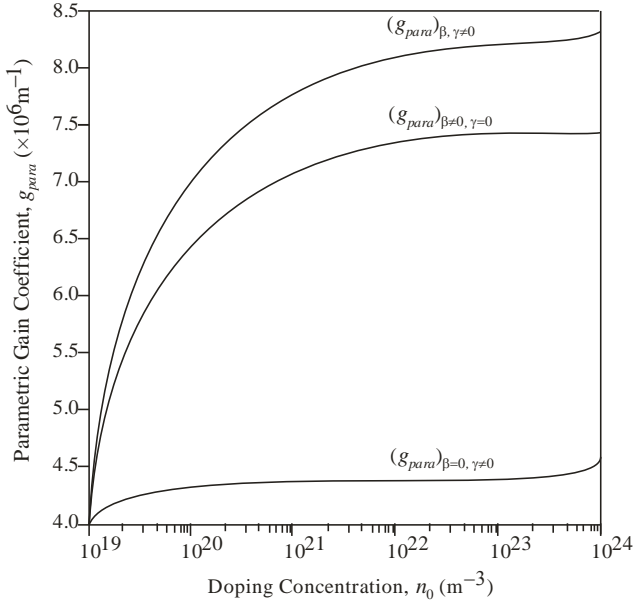


Fig. 6. Variation of parametric gain coefficients g_{para} with doping concentration n_0 for $B_0 = 14.2 T$

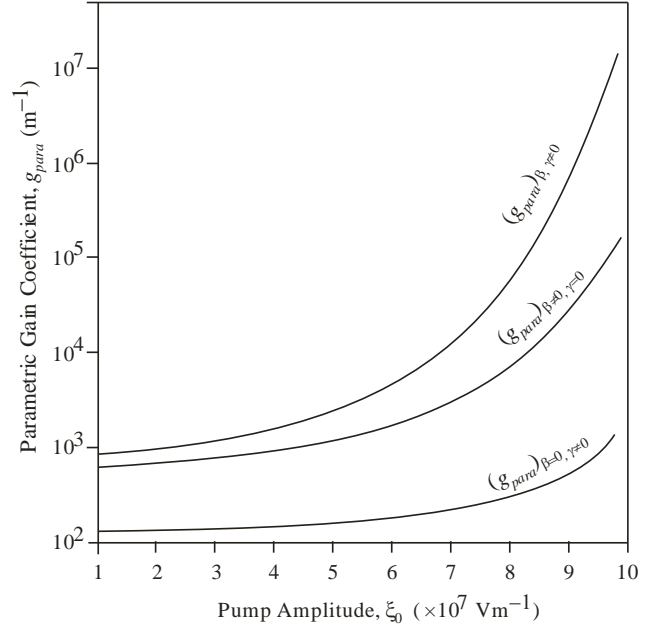


Fig. 7. Variation of parametric gain coefficients g_{para} with pump field amplitude ξ_0 for $n_0 \approx 10^{22} \text{ m}^{-3}$ and $B_0 = 14.2 T$

Fig. 7 shows the variation of parametric gain coefficients $((g_{para})_{\beta,\gamma \neq 0}, (g_{para})_{\beta=0,\gamma \neq 0}, (g_{para})_{\beta \neq 0,\gamma=0})$ with ξ_0 ($> \xi_{0,th}$) for $B_0 = 14.2 T$ and $n_0 \approx 10^{22} \text{ m}^{-3}$. We observed that the gain coefficients increases quadratically with increasing pump amplitude. Hence, high pump field amplitude yield larger gain coefficients. Here, it is worth mentioning that practically the pump field amplitude cannot be increased arbitrarily because it may optically damage the sample [34].

In Figs. 4-7, we observed that the parametric gain coefficient is largest in presence of both piezoelectricity and electrostriction both ($\beta \neq 0$ and $\gamma \neq 0$) while smallest in absence of piezoelectricity and presence of electrostriction ($\beta = 0$ and $\gamma \neq 0$) in anomalous and normal dispersion regimes of acoustic wave. In dispersion-less regime of acoustic wave, the gain coefficients becomes independent of type of (piezoelectric and/or electrostrictive) coupling. With $\xi_0 = 6 \times 10^7 \text{ Vm}^{-1}$, $B_0 = 14.2 T$, $n_0 \approx 10^{22} \text{ m}^{-3}$ and $\Omega_a \neq k_a v_a$, we obtained the following ratio:

$$(g_{para})_{\beta,\gamma \neq 0} : (g_{para})_{\beta \neq 0,\gamma=0} : (g_{para})_{\beta=0,\gamma \neq 0} = 1 : 2.5 \times 10^{-2} : 2.1 \times 10^{-4}$$

Table 3 shows the calculated values of parametric gain coefficient in n-InSb crystal.

Table 3. Calculated values of parametric gain coefficient in *n*-InSb crystal for $\xi_0 = 6 \times 10^7 \text{ Vm}^{-1}$

Parametric gain coefficient $g_{para} \text{ (m}^{-1}\text{)}$	Piezoelectric coefficient $\beta \text{ (Cm}^{-2}\text{)}$	Electrostrictive coefficient $\gamma \text{ (s}^{-1}\text{)}$	Magnetostatic field $B_0 \text{ (T)}$	Doping concentration $n_0 \text{ (m}^{-3}\text{)}$
2.5×10^3	0.054	5×10^{-10}	0	10^{22}
6.5×10^2	0.054	0	0	10^{22}
1.5×10^2	0	5×10^{-10}	0	10^{22}
6.5×10^4	0.054	5×10^{-10}	11	10^{22}
8.5×10^3	0.054	0	11	10^{22}
7.5×10^2	0	5×10^{-10}	11	10^{22}
4.0×10^7	0.054	5×10^{-10}	14.2	10^{22}
1.0×10^6	0.054	0	14.2	10^{22}
8.5×10^3	0	5×10^{-10}	14.2	10^{22}

4. Conclusions

In the present study, using the fluid model of semiconductor plasmas and adopting the coupled mode approach, the role of piezoelectric and electrostrictive coupling on threshold and gain coefficient of OPA of APs in magnetized doped III-V semiconductors have been undertaken. The proper selection of an externally applied magnetostatic field (around resonance conditions) plays a critical role in reducing the threshold pump field in dispersion-less regime of acoustic wave. Moreover, the high doping concentration is favourable for lowering the threshold pump amplitude for the onset of OPA. The parametric gain coefficients can be resonantly enhanced by properly adjusting the externally applied magnetostatic field. The parametric gain coefficient is largest in presence of both piezoelectricity and electrostriction both while smallest in absence of piezoelectricity and presence of electrostriction in anomalous and normal dispersion regimes of acoustic wave. In dispersion-less regime of acoustic wave, the gain coefficients becomes independent of type of (piezoelectric and/or electrostrictive) coupling. The technological potentiality of a magnetized weakly piezoelectric doped semiconductor as the hosts for parametric devices like parametric amplifiers and optical switches are established. In III-V semiconductor crystals, OPA in the infrared regime appears quite promising under the resonance conditions and replaces the conventional idea of using high power pulsed lasers.

Acknowledgements

One of the authors (M. Singh) is thankful to Director General, Department of Higher Education, Haryana for kind cooperation to carry out this research work.

References

- [1] T. Kobayashi, J. Liu, K. Okamura, *J. Phys. B: At. Mol. Opt. Phys.* **45**, 074005 (2012).
- [2] M. E. Marhic, P. A. Andrekson, P. Petropoulos, S. Radic, C. Peucheret, M. Jazayerifar, *Laser Photon. Rev.* **9**, 50 (2015).
- [3] Jing Huang, *Parametric Amplifiers in Optical Communication Systems: From Fundamentals to Applications*, Optical Amplifiers - A Few Different Dimensions, P. K. Choudhury, (Intech Open, 2018).
- [4] P. K. Loharkar, A. Ingle, S. Jhavar, *J. Mat. Res. Chem.* **8**, 3306 (2019).
- [5] D. Brida, C. Manzoni, G. Cirimi, M. Marangoni, S. de Silvestri, *Opt. Exp.* **15**, 15035 (2007).
- [6] K. Nawata, Y. Tokizane, Y. Takida, H. Minamide, *Sci. Rep.* **9**, 726 (2019).
- [7] Z. Tong, S. Radic, *Adv. Opt. Photonics* **5**, 318 (2013).
- [8] M. E. Marhic, P. A. Andrekson, P. Petropoulos, S. Radic, C. Peucheret, M. Jazayerifar, *Laser Photon Rev.* **9**, 50 (2015).
- [9] Y. Sun, H. Tu, S. You, C. Zhang, Y. Z. Liu, S. A. Boppart, *Opt. Lett.* **44**, 4391 (2019).
- [10] D. Arivuoli, Pramana, *J. Phys.* **57**, 871 (2001).
- [11] S. J. Sweeney, J. Mukherjee, *Optoelectronic Devices and Materials*. In: S. Kasap, P. Capper(eds) Springer Handbook of Electronic and Photonic Materials, Springer Handbooks, 2017.
- [12] S. Mokkalapati, C. Jagadish, *Materials Today* **12**, 22 (2009).
- [13] S. Ghosh, S. Khan, *Ultrasonics* **24**, 93 (1986).
- [14] P. K. Gupta, P. K. Sen, *Nonlinear Opt.* **26**, 361 (2001).
- [15] M. Singh, P. Aghamkar, S. K. Bhakar, *Opt. Laser Tech.* **41**, 64 (2009).
- [16] B. Lal, P. Aghamkar, *J. Mod. Phys.* **2**, 771 (2011).
- [17] S. Ghosh, G. Sharma, M. P. Rishi, *Physica B: Cond. Matter* **328**, 255 (2003).
- [18] S. K. Ghosh, G. Sharma, P. Khare, M. Salimullah, *Physica B: Cond. Matter* **351**, 163 (2004).

- [19] S. K. Ghosh, P. Thakur, N. Yadav, M. Salimullah, Arabia J. Sci. Eng. **35**, 0231 (2010).
- [20] G. Manfredi, Fields Inst. Commun. **46**, 263 (2005).
- [21] A. Rasheed, M. Jamil, M. Siddique, F. Huda, Y. D. Jung, Phys. Plasmas **21**, 062107 (2014).
- [22] F. Haas, Phys Plasmas **12**, 062117 (2005).
- [23] M. Marklund, P. K. Shukla Rev. Mod. Phys. **78**, 591 (2006).
- [24] M. A. Moghanjoughi, Phys. Plasmas. **18**, 012701 (2011).
- [25] F. Hass, A. Bret, Europhys. Lett. **97**, 26001 (2012).
- [26] S. Ghosh, S. Dubey, R. Vanshpal, Chin. J. Phys. **51**, 1251 (2013).
- [27] S. Ghosh, S. Dubey, R. Vanshpal, Phys. Lett. A **375**, 43 (2010).
- [28] M. Singh, P. Aghamkar, S. Duhan, Chin. Phys. Lett. **25**, 327 (2008).
- [29] M. Singh, Physica B: Cond. Matter **403**, 3985 (2008).
- [30] D. L. Spears, Phys. Rev. B **2**, 1931 (1970).
- [31] J. J. Wynne, N. Bloembergen, Phys. Rev. **188**, 1211 (1969).
- [32] E. R. Generazio, H.N. Spector, Phys. Rev. B **20**, 5162 (1979).
- [33] E. D. Pilak, J. K. Furdyna, Rep. Prog. Phys. **33**, 1193 (1970).
- [34] J. M. Mayer, F. J. Bartoli, M. R. Kruer, Phys. Rev. B **21**, 1559 (1980).

*Corresponding author: msgur_18@yahoo.com